

42. MAGNETOSTRATIGRAPHY OF UPPER CRETACEOUS AND LOWER TERTIARY SEDIMENTS, SITES 761 AND 762, EXMOUTH PLATEAU, NORTHWEST AUSTRALIA¹

Bruno Galbrun²

ABSTRACT

Lower Campanian to middle Eocene chalks and oozes were recovered at Sites 761 and 762 of Ocean Drilling Program Leg 122 on the Exmouth Plateau, northwest Australia. Paleomagnetic analyses were made on 125 samples from Hole 761B and 367 samples from Hole 762C. Thermal cleaning, alternating field demagnetization, or mixed treatment reveals a stable remanent component of normal or reversed polarity. Correlation of the magnetic polarity sequences established for these holes with the standard magnetic polarity time scale was aided by nannofossil zonation. At Hole 761B, the sequence extends from Subchron C32-N (upper Campanian) through Subchron C17-R (middle Eocene), but given the low sedimentation rate, not all the subchrons of the standard magnetic polarity sequence were recognized. The sequence at Hole 762C extends from Subchron C13-R (middle Eocene) to the boundary between Chrons C33 and C34 (lower Campanian). The sedimentation rate is higher at Hole 762C, and all the magnetic polarity subchrons of the Campanian and Maestrichtian stages were identified. Thus, this hole could be a reference section to refine the Upper Cretaceous time scale.

INTRODUCTION

Site 762 of Ocean Drilling Program (ODP) Leg 122 was cored on the western part of the central Exmouth Plateau (northwest Australia) at 19°53'S, 112°15'E (Fig. 1). Site 761 was drilled at 16°44'S, 115°32'E, on the central part of Wombat Plateau, which is a small subplateau on the northern edge of Exmouth Plateau (Fig. 1). A 160-m-thick section of upper Campanian to middle Eocene pelagic carbonates was cored from Hole 761B with an excellent recovery except for Cores 122-761B-13C and -15C (lower-middle Eocene). From Hole 762C, a very thick (550 m) section of lower Campanian to middle Eocene chalks and oozes was cored with good recovery.

Some of the major objectives of Leg 122 were (1) to study the Cretaceous to Cenozoic post-breakup development of sedimentation and paleoenvironment from a "juvenile" to a "mature" ocean, and (2) to study the temporal and spatial distribution of Mesozoic and Cenozoic sediments and thus allow the testing of the eustatic sea-level curve (Haq et al., 1987). For these objectives very precise age constraints are necessary and could be obtained by joint biostratigraphic and magnetostratigraphic studies. As a matter of fact, the Upper Cretaceous and Cenozoic biostratigraphic time scale is now well correlated with the magnetic polarity time scale (Haq et al., 1987, 1988).

Various studies have shown that pelagic sediments recovered during Deep Sea Drilling Project (DSDP) and ODP yielded excellent magnetostratigraphic results (Hamilton and Suzyumov, 1983; Chave, 1984; Petersen et al., 1984; Tauxe et al., 1984; Ogg, 1987). This paper presents the magnetostratigraphic results of Upper Cretaceous-lower Tertiary sequences from Holes 761B and 762C.

METHODS

The natural remanent magnetization (NRM) and remanence after 9-millitesla (mT) alternating field (AF) demagnetization of all archive core halves were measured on board with the 2G-Enterprises 760R cryogenic magnetometer at 10- or 5-cm intervals. But this procedure was not effective for determining the magnetostratigraphy of relatively old pelagic sediments given the weak NRM intensity and the viscous remanent magnetization (VRM) of the Earth's present field direction overprint which could not be removed by the 9-mT AF demagnetization. Thus, extended sampling for shore-based analysis was carried out.

Two paleomagnetic samples were taken from each 1.5-m section of recovered sedimentary rock. The soft oozes were sampled by pushing oriented plastic boxes (7 cm³) from the working half of the split core; the resulting sample was removed with a spatula. Some indurated chalks were sampled using a drill press by drilling 11 cm³ minicores (2.5-cm diameter, 2.4-cm length) perpendicular to the axis of the core.

Most of the samples were weakly magnetized, and all were measured with a 3-axis RS-01 (LETI/CEA) cryogenic magnetometer in the Département de Géologie Sédimentaire, Université Paris VI. The sensitivity of this instrument is such that it could measure magnetized samples as weak as 2×10^{-5} A/m with good precision. All samples were subjected to progressive demagnetization. Such usual techniques as thermal demagnetization, AF demagnetization, or mixed treatment (thermal and subsequent AF) were used to isolate primary remanence components. The magnetic mineralogy and properties of deep-sea marine limestones are now well known (Lowrie and Heller, 1982; Freeman, 1986; Galbrun and Butler, 1986), and it is assumed that moderate demagnetization is sufficient to remove soft secondary magnetic overprints in pelagic limestones. The directions of characteristic remanent magnetization (ChRM) of single samples were determined by least squares analysis to vectors in the region of linear decay toward the origin of the vector plot (Kirschvink, 1980) using the software of Torsvik (1986). Some samples could not be demagnetized at high steps, mainly given their NRM intensity weakness, and do not reach a linear decay to the origin of the

¹ von Rad, U., Haq, B. U., et al., 1992. Proc. ODP, Sci. Results, 122: College Station, TX (Ocean Drilling Program).

² Université Paris VI, Département de Géologie Sédimentaire, UA-CNRS 1315, 4 place Jussieu, 75252 Paris Cedex 05, France.

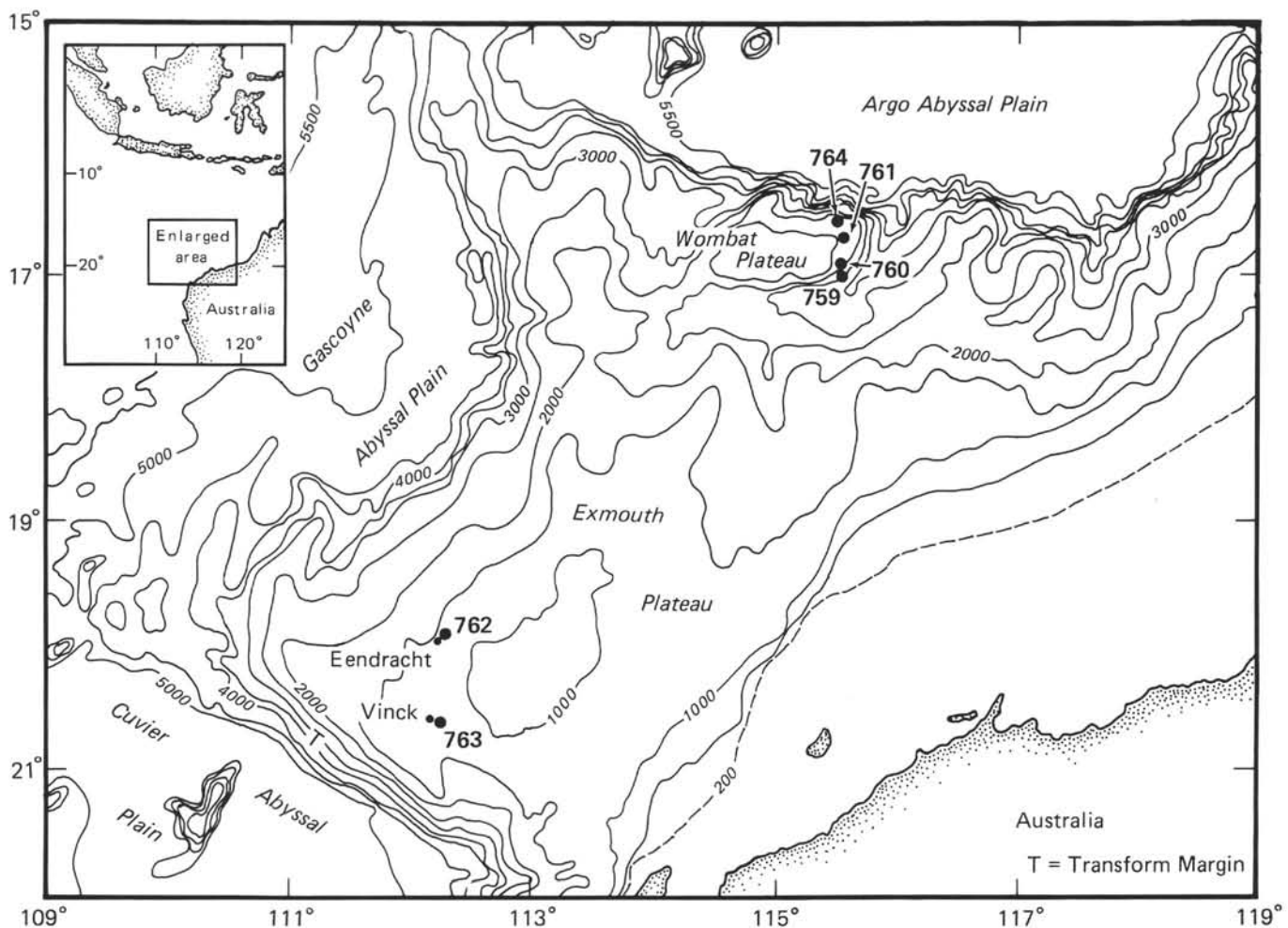


Figure 1. Bathymetric map of Exmouth Plateau with location of Leg 122 sites. Bathymetry in meters.

vector plot. Thus, their ChRM direction was defined as the last direction measured with good precision.

Some very weakly magnetized samples have a NRM intensity so weak (less than 2×10^{-5} A/m) that they could not be measured with good precision; nevertheless a progressive demagnetization was tried on these samples. Some of them, of reversed polarity presented an increasing of intensity during the removal of the normal overprint, only such samples were considered.

The Leg 122 cores were not oriented horizontally, thus only magnetic inclination could be used to indicate polarity. Upper Cretaceous-lower Tertiary sediments recovered from Holes 761B and 762C were deposited at middle to high paleolatitudes and inclination data alone are adequate. The Exmouth Plateau is in the Southern Hemisphere, and thus positive inclinations result from a reversed field.

MAGNETIC PROPERTIES AND MAGNETOSTRATIGRAPHY

Hole 761B

One-hundred twenty-five samples were collected from Core 122-761B-8H (middle Eocene) to Core 122-761B-25X (upper Campanian). The sediments are mainly white nannofossil chalks or white nannofossil oozes (Shipboard Scientific Party, 1990a). The NRM intensities range from less than 10^{-5} to 9.9×10^{-3} A/m.

The NRM intensity curve shows a decrease from Cores 122-761B-20X to -23X. The most weakly magnetic sample was 122-761B-21X, 113 cm (lower Paleocene), which had an NRM intensity of 9×10^{-6} A/m. But there is no correlation between variations of NRM intensity and lithologic units.

The magnetic characteristics of white chalks and white oozes are generally similar and thus, only five pilot samples were selected for detailed AF demagnetization. Each specimen was demagnetized at 5, 10, 15, 20, 25, 30, and 35 mT. A first soft component was removed in 15 mT peak fields and a stable component was defined between about 15 and 35 mT (Fig. 2, Sample 122-761B-35X-2, 76 cm). But given acquisition of anhysteretic remanent magnetization components caused by the demagnetizer in most weak magnetized samples, the AF technique could not be used as a routine technique. Seventeen pilot samples were thermally demagnetized in 50° steps from 100°C up to 500°C. This treatment was effective: an initial unstable component was removed by 150°–200°C and the ChRM direction was clearly defined above these temperatures (Fig. 2, Sample 122-761B-18X-4, 49 cm). Meanwhile, thermal demagnetization could not be used as a routine technique because most of the samples were in plastic boxes and could not be heated at high temperature. Thus, eight minicores were heated at 300°C and AF demagnetized, and all the remaining samples (95 plastic boxes) were treated at 100°C and 10, 15, 20, 25, 30, and 35 mT. This mixed cleaning was

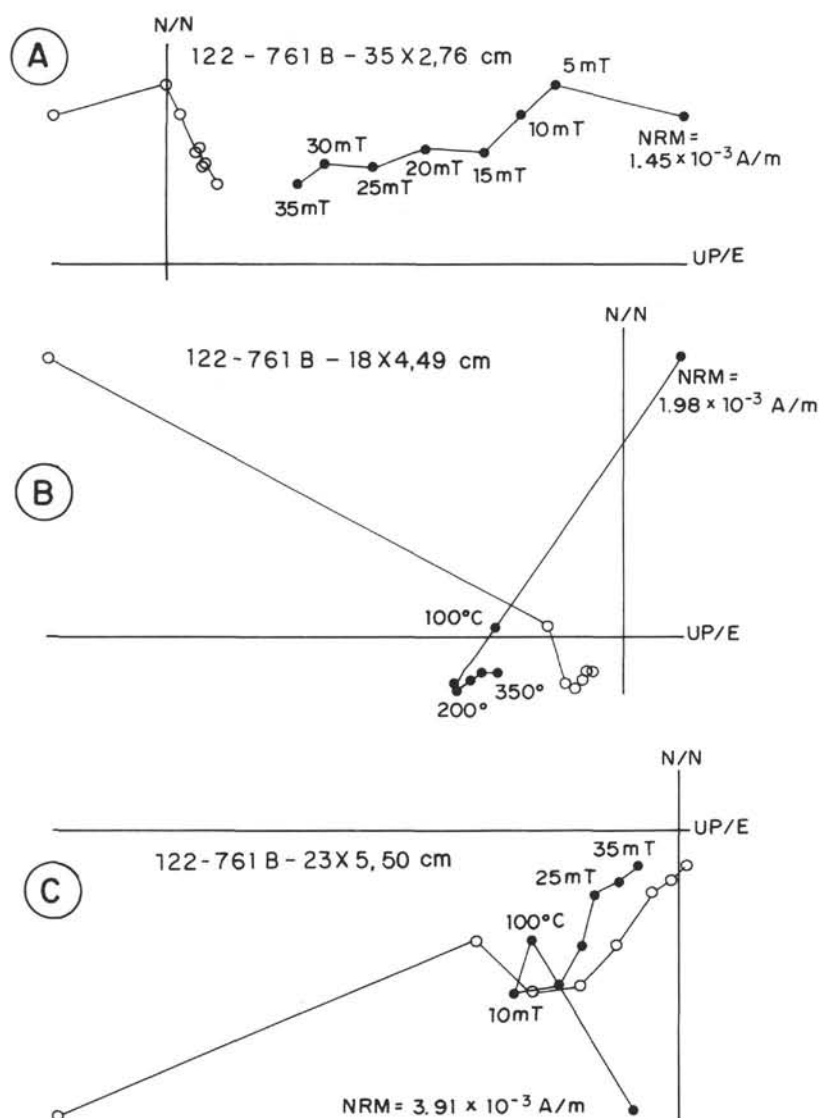


Figure 2. Orthogonal vector plots of demagnetization curves for typical samples from Hole 761B. A. AF demagnetization. B. Thermal demagnetization. C. Mixed treatment (heating at 100°C and subsequent alternating field demagnetization). Solid (open) circles denote projection in the vertical (horizontal) plane. The initial declination is arbitrary because orientation control is lacking.

also very effective in isolating a stable component (Fig. 2, Sample 122-761B-23X-5, 50 cm).

The first soft component is of negative inclination (normal polarity) and is interpreted as a VRM due to Earth's present field. The stable component is of positive or negative inclination and thus is most probably a primary component of reversed or normal polarity. The inclination values of this stable component present a good bimodal distribution (Fig. 3). Some weakly magnetized samples were completely demagnetized by 100°C heating: ChRM directions could not be computed from these samples but their polarity is believed to represent a primary component.

The primary component directions give a good magnetic polarity stratigraphy (Fig. 4). Correlations with biostratigraphic data, based on nannofossil zonation (Bralower and Siesser, this volume; Siesser and Bralower, this volume) allow tentative assignments to the standard magnetic polarity time

scale (Haq et al., 1987). The magnetic polarity sequence extends from Subchron C32-N (upper Campanian) to Subchron C17-R (middle Eocene). Some polarity zones are recognized by single samples, especially when the sedimentation rate is low, such as just above the Cretaceous-Tertiary boundary (Chrons C29 and C28). A single sample of normal polarity occurs within the reversed Subchron C26-R, it could correspond to a short subchron as already noted at DSDP Site 524 (Tauxe et al., 1984). An additional sampling of cores from Hole 761B will probably allow satisfactory recognition of some standard magnetic polarity zones.

Hole 762C

Three-hundred sixty-seven samples were analyzed from Core 122-762C-5X (middle Eocene, NP20 nannofossil zone) to Core 122-762C-6X (lower Campanian). The lithology consists of nannofossil chalks and some clay-rich nannofossil

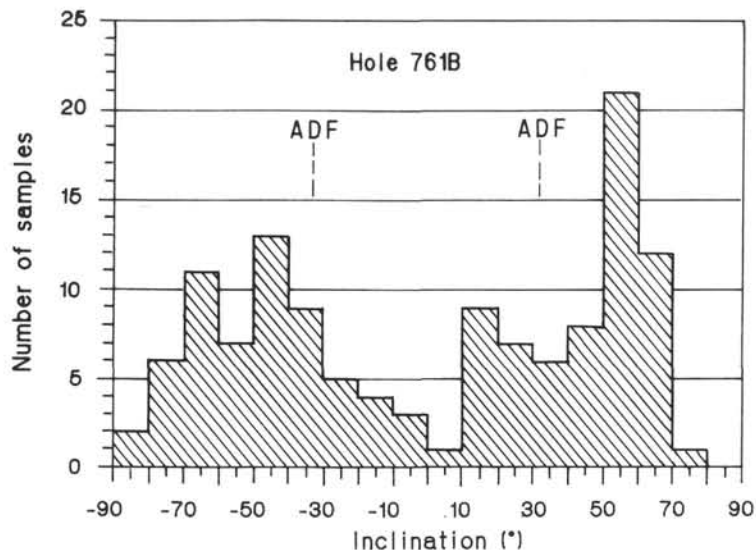


Figure 3. Histogram of paleo-inclination values of Hole 761B. ADF indicates axial dipole field inclination for actual site latitude. The positive and negative inclination values present a good bimodal distribution.

chalks to claystones in the upper Cretaceous (Shipboard Scientific Party, 1990b). The NRM intensities of nannofossil chalks were generally low, ranging from 4×10^{-6} to 9×10^{-4} A/m. The Cores 122-762C-11X to -21X are more strongly magnetized, up to 8.7×10^{-3} A/m. This variation does not correspond to a lithological change, and a coring disturbance is suspected. The clayey nannofossil chalks and claystones of Subunits IVa, b, and c (Upper Cretaceous) displayed strong NRM's, especially in the clayey chalks and claystones of Subunit IVb where NRM intensities were found between 10^{-4} to 3.9×10^{-2} A/m.

Pilot samples of different lithologies and various NRM intensities were subjected to detailed demagnetization (Fig. 5). Twelve pilot samples were cleaned by AF demagnetization. Peak field increments of 5 mT were used up to 60 mT. This treatment was effective in removing a low coercivity component and in isolating a stable component above 15 mT. Eighteen pilot samples were thermally demagnetized in 50° steps up to 500°C. An initial unstable component was removed by 200°C. The characteristic remanent magnetization direction was clearly defined above this temperature and 49 samples were heated at a selected set of about four or five steps between 250° and 500°C depending on the NRM intensities. The first unstable component of negative inclination is most probably a secondary viscous magnetization while the stable component of positive or negative inclination is the primary magnetization.

Given that both treatments were effective, a mixed cleaning was chosen for all the remaining samples: 150°C and AF demagnetization for indurated minicore samples, 100°C and AF treatment for soft samples in plastic boxes. But many of the samples from Hole 762C were weakly magnetized and could be demagnetized only at 100°C or 100°C and 10 mT. Characteristic magnetization directions could not be computed by least squares analysis from these samples, but their polarity is thought to be original and their ChRM direction was defined as the last step measured with good precision.

The ChRM directions computed or defined at a specific demagnetization step present clearly bimodal distributions of positive and negative inclination values in most parts of the hole (Fig. 6A, -B).

Strongly magnetized chalks from Cores 122-762C-11X to -21X presented a lower value of inclination before treatment and had a different behavior during demagnetization. Most of the NRM was rapidly removed by 100°C heating and 15 mT. Above this value, the ChRM direction seems defined (Fig. 5, Samples 122-762C-19X-2, 30 cm, and 122-762C-20X-1, 131 cm). But these ChRM directions display low values of inclination which are positive and negative and do not present a bimodal distribution (Fig. 6C). Thus the NRM of Cores 122-762C-11X to -21X seems dominated by a secondary component not completely removed during the demagnetization. This component could be induced by the drilling as sometimes observed (Jackson and Van der Voo, 1985; Pinto and McWilliams, 1990). We do not have real arguments to assert this fact, and we can only note that this part of the hole corresponds to the higher penetration rate during the drilling of Hole 762C: this rate increases suddenly between Cores 122-762C-10X and -11X and decreases suddenly between Cores 122-762C-21X and -22X (Shipboard Scientific Party, 1990b, p. 220, fig. 7). These changes in penetration rates coupled with changes in magnetic properties do not correspond to lithological variations.

The magnetostratigraphic results are presented in Figure 7. Referring to the calcareous nannofossil biostratigraphy (Bralower and Siesser, this volume; Siesser and Bralower, this volume), correlations with the geomagnetic polarity time scale seem unambiguous for the Cores 122-762C-5X to -10X (upper part of middle Eocene) and Cores 122-762C-22X to -62X (lower Eocene to lower Campanian). We are less confident with the correlations of Cores 122-762C-11X to -21X. The polarity sequence extends from Subchron C13-R (middle Eocene) to the boundary between Chrons C33 and C34 (lower Campanian).

CONCLUSIONS

Preliminary analysis of the lower Campanian to middle Eocene nannofossil chalks and oozes of Sites 761 and 762 give good magnetostratigraphic results. The secondary remanence overprint was generally easily removed from each sample by moderate thermal, alternating field demagnetization, or mixed treatment, all except the Cores 122-762C-11X to -21X.

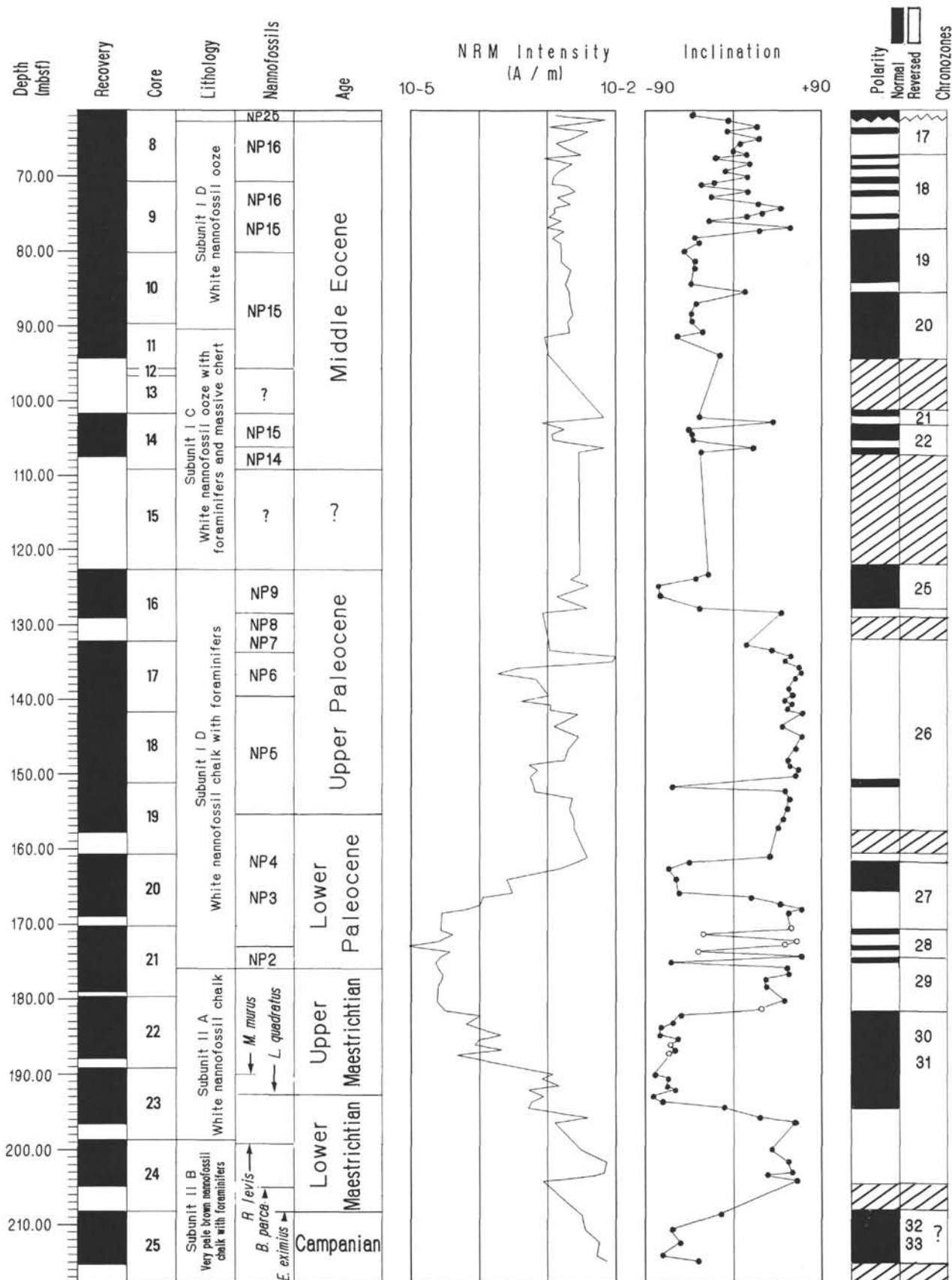


Figure 4. Magnetostratigraphic results from Hole 761B, showing sub-bottom depth, recovery (black), cores, lithological units, nannofossil zones, age, NRM intensity, inclination (samples which could not be demagnetized at high steps, given their weakness of NRM intensity, are represented by open circles), polarity interpretation, and a suggested assignment to polarity chrons (magnetic polarity time scale of Haq et al., 1987).

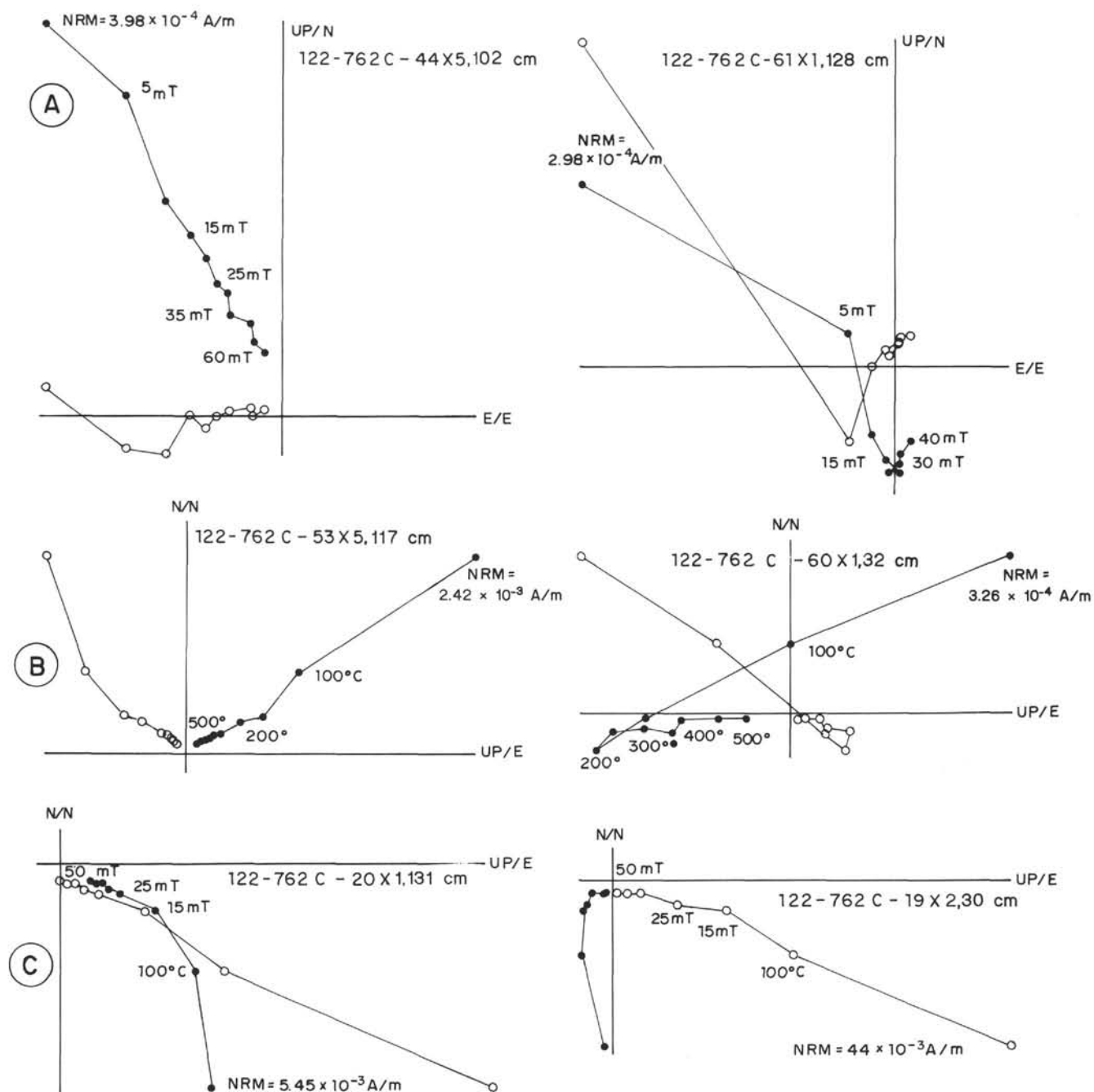


Figure 5. Vector demagnetization plots of samples from Hole 762C. A. AF demagnetization. B. Thermal demagnetization. C. Mixed treatment on strongly magnetized chalks from Cores 122-762C-11X to -21X. Solid (open) circles denote projection in the vertical (horizontal) plane. The initial declination is arbitrary because orientation control is lacking.

We refer to the calcareous nannofossil zonation to identify the magnetic polarity chronos, and possible correlations to the magnetic polarity time scale (Haq et al., 1987) are presented on Figures 4 and 7, for Holes 761B and 762C, respectively. Given low sedimentation rate and bad recovery at Hole 761B, not all magnetic polarity zones of the standard succession were recognized. Given good recovery at Hole 762C coupled with high sedimentation rate, the magnetostratigraphic results obtained at this hole are excellent: most of the Chrons C33 through C13 are identified (Fig. 8). Thus, this hole is one of the

most documented section of its age, and should be a reference section for the Indian Ocean.

ACKNOWLEDGMENTS

I thank the Ocean Drilling Program for allowing my participation on Leg 122. This study was supported by ODP-France and the CNRS-UA 1315. The manuscript was reviewed by S. O'Connell, N. Petersen, and two anonymous reviewers. I am grateful to J. Thompson for revision of the English.

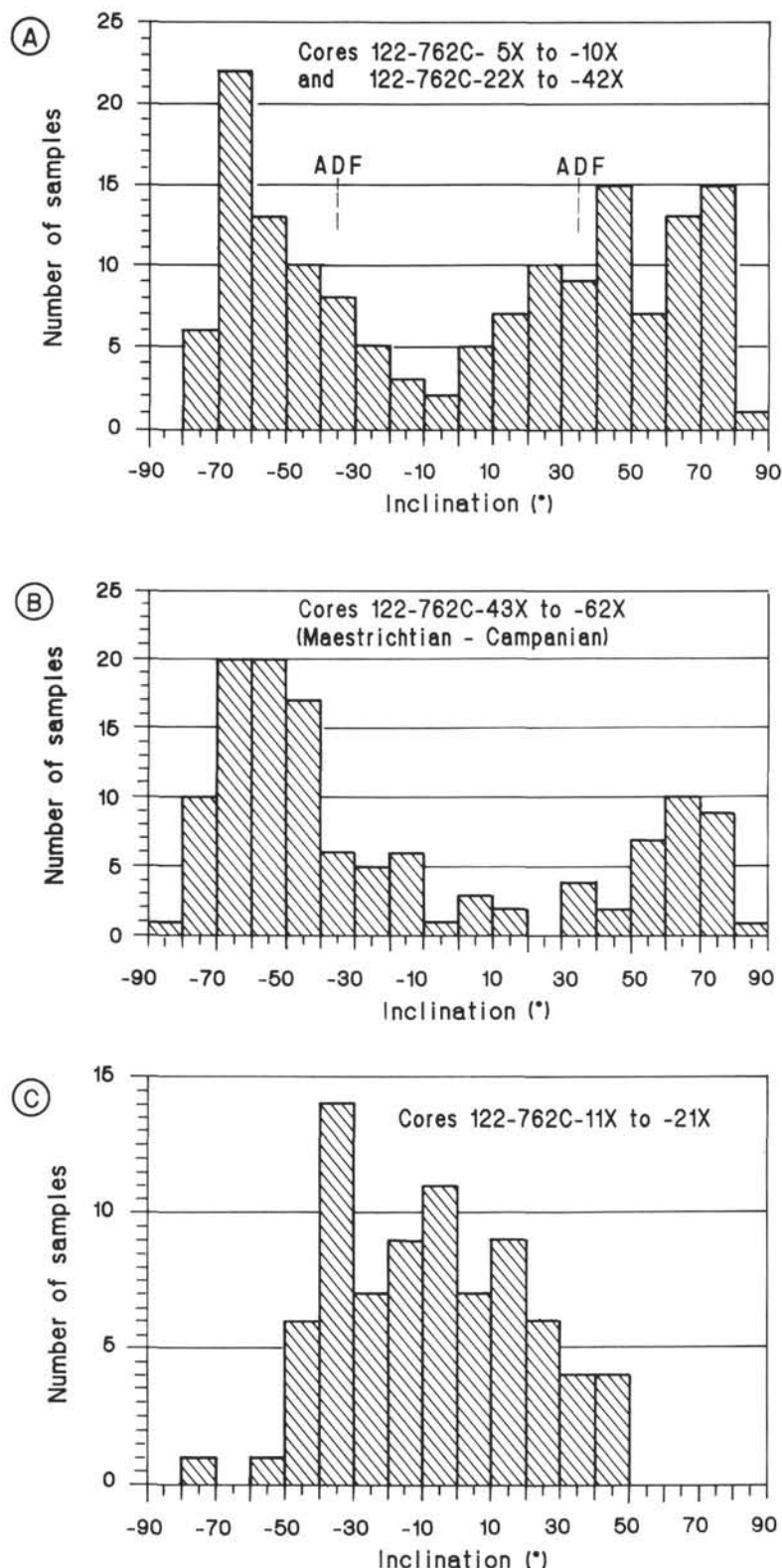


Figure 6. Histograms of paleo-inclination values of Hole 762C. ADF indicates axial dipole field inclination for actual site latitude. **A.** Good bimodal clustering of inclination values in Cenozoic samples from Cores 122-762C-5X to -10X and Cores 122-762C-22X to -42X. **B.** Good bimodal distribution of inclination values of Upper Cretaceous samples from Cores 122-762C-43X to -62X. **C.** Large scatter of strongly magnetized samples from Cores 122-762C-11X to -21X; this large scatter is due to the incomplete removal of the secondary component acquired in this part of the hole possibly during the drilling.

REFERENCES

- Chave, A. D., 1984. Lower Paleocene–Upper Cretaceous magnetostratigraphy, Sites 525, 527, 528, and 529, Deep Sea Drilling Project Leg 74. In Moore, T. C., Jr., Rabinowitz, P. D., et al., *Init. Repts. DSDP*, 74: Washington (U.S. Govt. Printing Office), 525–531.
- Freeman, R., 1986. Magnetic mineralogy of pelagic limestones. *Geophys. J. R. Astron. Soc.*, 85:433–452.
- Galbrun, B., and Butler, R. F., 1986. Curie temperature analyses of upper Jurassic and lower Cretaceous pelagic limestones. *Geophys. J. R. Astron. Soc.*, 86:885–892.
- Hamilton, N., and Susyumov, A. E., 1983. Late Cretaceous magnetostratigraphy of Site 516, Rio Grande Rise, southwestern Atlantic Ocean, Deep Sea Drilling Project, Leg 72. In Barker, P. F., Carlson, R. L., Johnson, D. A., et al., *Init. Repts. DSDP*, 72: Washington (U.S. Govt. Printing Office), 723–730.
- Haq, B. U., Hardenbol, J., and Vail, P. R., 1987. Chronology of fluctuating sea levels since the Triassic. *Science*, 235:1156–1167.
- _____, 1988. Mesozoic and Cenozoic chronostratigraphy and cycles of sea-level change. In Wilgus, C. K., Hastings, B. S., Kendall, C.G.St.C., Posamentier, H. W., Ross, C. A., and Van Wagoner, J. C. (Eds.), *Sea-Level Changes—An Integrated Approach*. Spec. Publ.—Soc. Econ. Paleontol. Mineral., 42:71–108.
- Jackson, M., and Van der Voo, R., 1985. Drilling-induced remanence in carbonate rocks: occurrence, stability and grain-size dependence. *Geophys. J. R. Astron. Soc.*, 81:75–87.
- Kirschvink, J. L., 1980. The least-squares line and plane and analysis of palaeomagnetic data. *Geophys. J. R. Astron. Soc.*, 62:699–718.
- Lowrie, W., and Heller, F., 1982. Magnetic properties of marine limestones. *Rev. Geophys. Space Phys.*, 20:171–192.
- Ogg, J. G., 1987. Early Cretaceous magnetic polarity time scale and the magnetostratigraphy of Deep Sea Drilling Project Sites 603 and 534, Western Central Atlantic. In van Hinte, J. E., Wise, S. W., Jr., et al., *Init. Repts. DSDP*, 93: Washington (U.S. Govt. Printing Office), 849–879.
- Petersen, N. P., Heller, F., and Lowrie, W., 1984. Magnetostratigraphy of the Cretaceous/Tertiary geological boundary. In Hsü, K. J., LaBrecque, J. L., et al., *Init. Repts. DSDP*, 73: Washington (U.S. Govt. Printing Office), 657–661.
- Pinto, M. J., and McWilliams, M., 1990. Drilling-induced isothermal remanent magnetization. *Geophysics*, 55:111–115.
- Shipboard Scientific Party, 1990a. Site 761. In Haq, B. U., von Rad, U., O'Connell, S., et al., *Proc. ODP, Init. Repts.*, 122: College Station, TX (Ocean Drilling Program), 161–211.
- _____, 1990b. Site 762. In Haq, B. U., von Rad, U., O'Connell, S., et al., *Proc. ODP, Init. Repts.*, 122: College Station, TX (Ocean Drilling Program), 213–288.
- Tauxe, L., Tucker, P., Petersen, N. P., and LaBrecque, J. L., 1984. Magnetostratigraphy of Leg 73 sediments. In Hsü, K. J., LaBrecque, J. L., et al., *Init. Repts. DSDP*, 73: Washington (U.S. Govt. Printing Office), 609–621.
- Torsvik, T. H., 1986. IAPD—Interactive Analysis of Palaeomagnetic Data. Univ. of Bergen, Inst. of Geophys., internal publication.

Date of initial receipt: 5 June 1990

Date of acceptance: 2 March 1991

Ms 122B-149

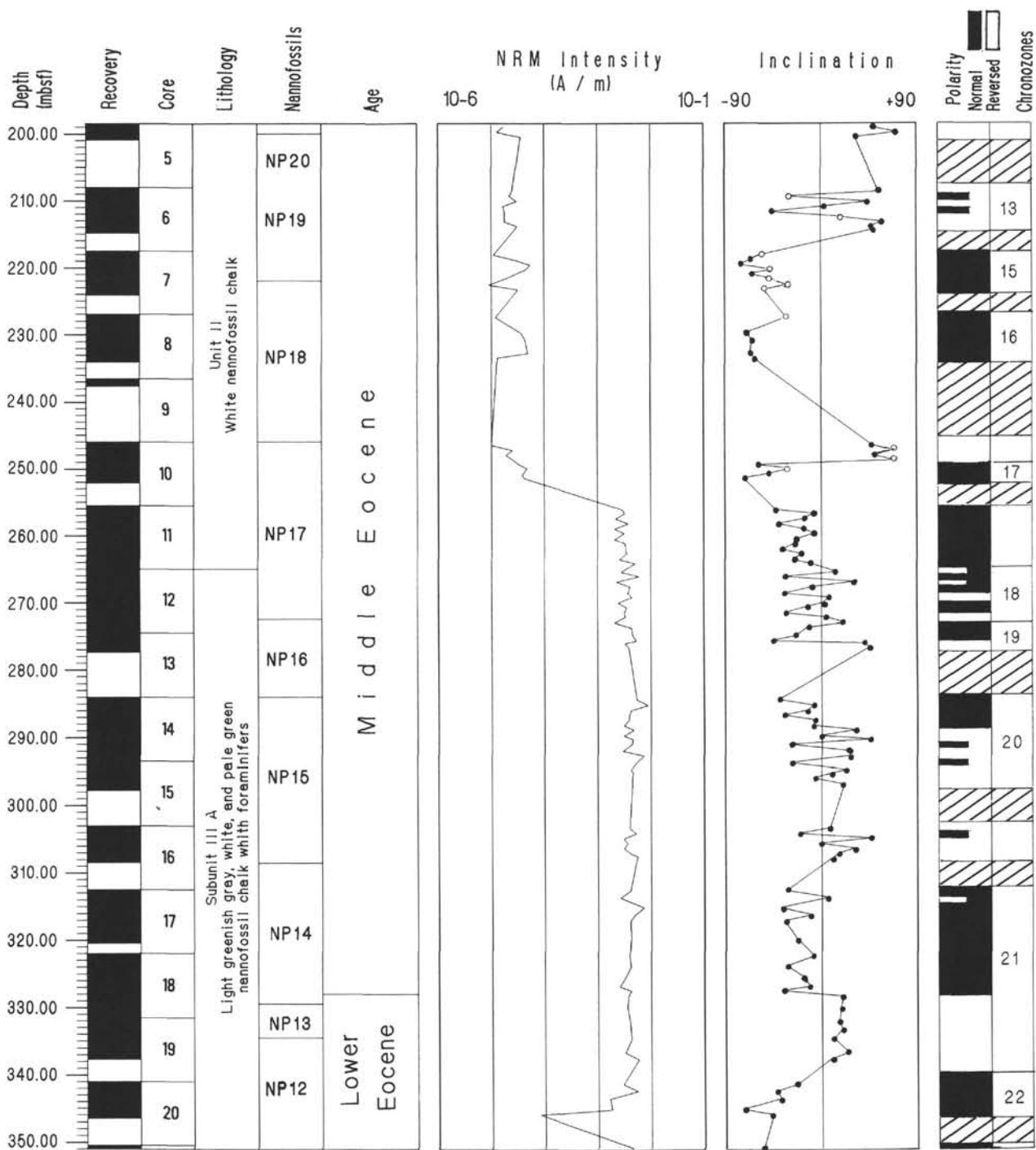


Figure 7. Magnetostratigraphic results from Hole 762C (see Fig. 4 caption for details).

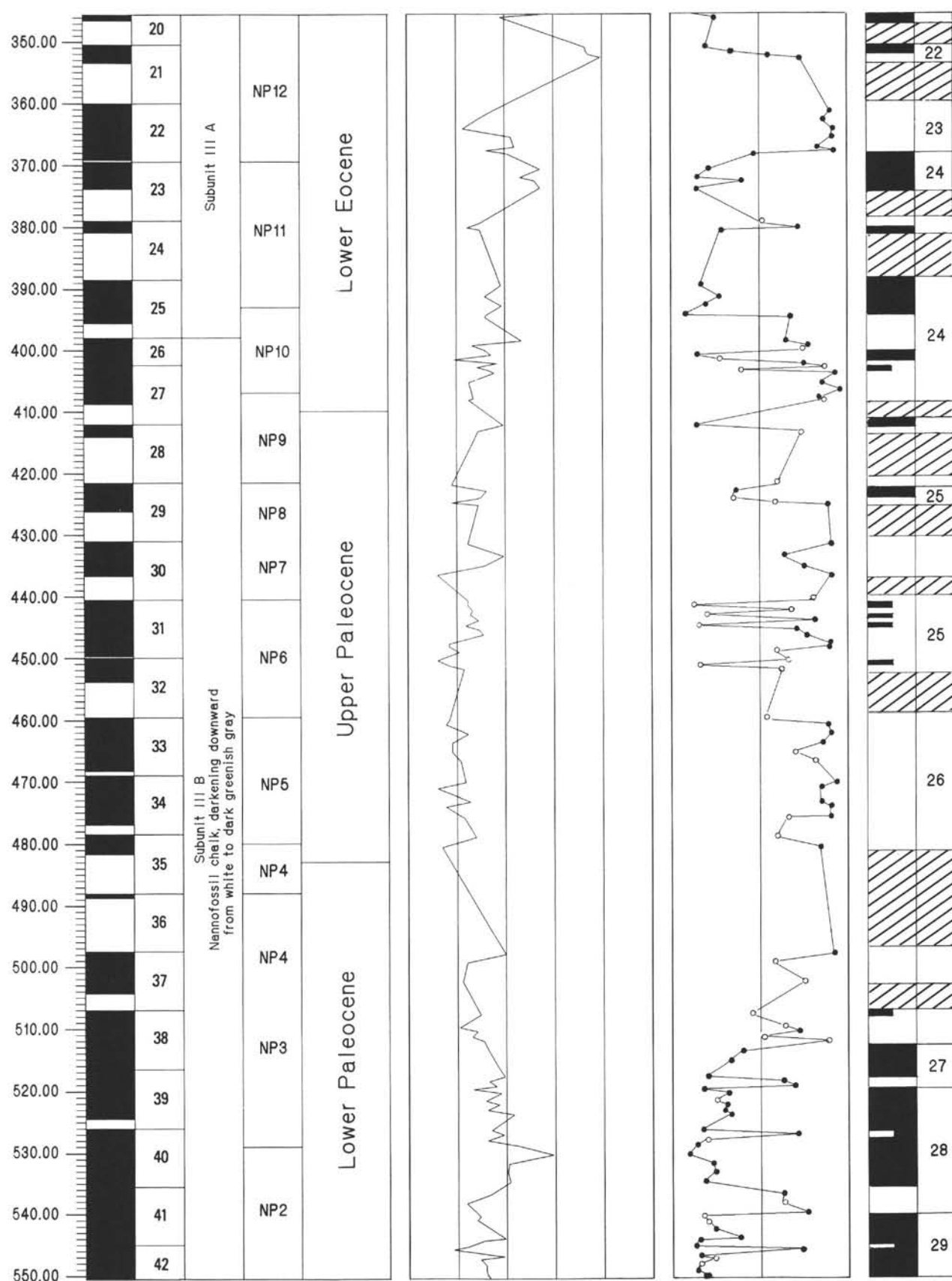


Figure 7 (continued).

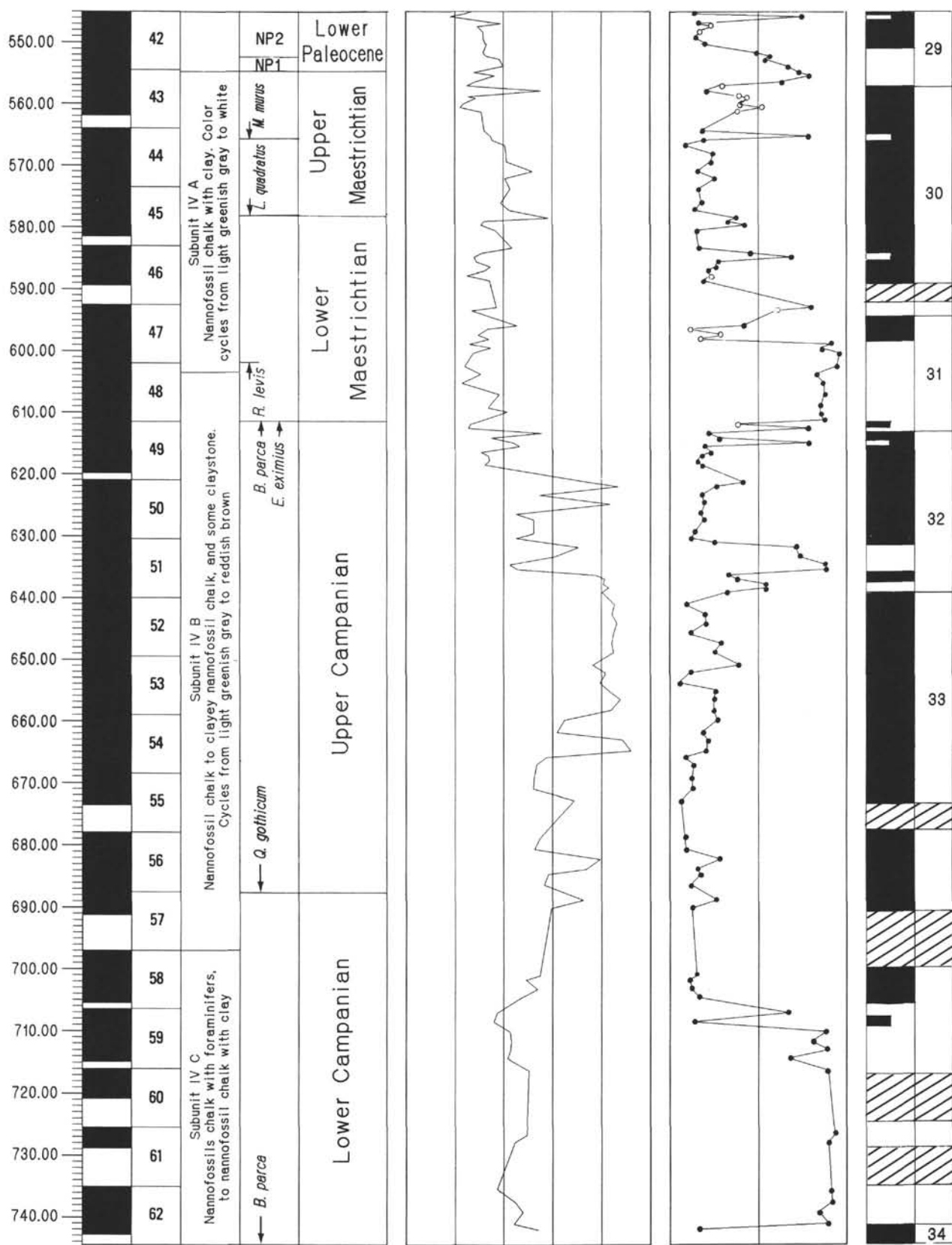


Figure 7 (continued).

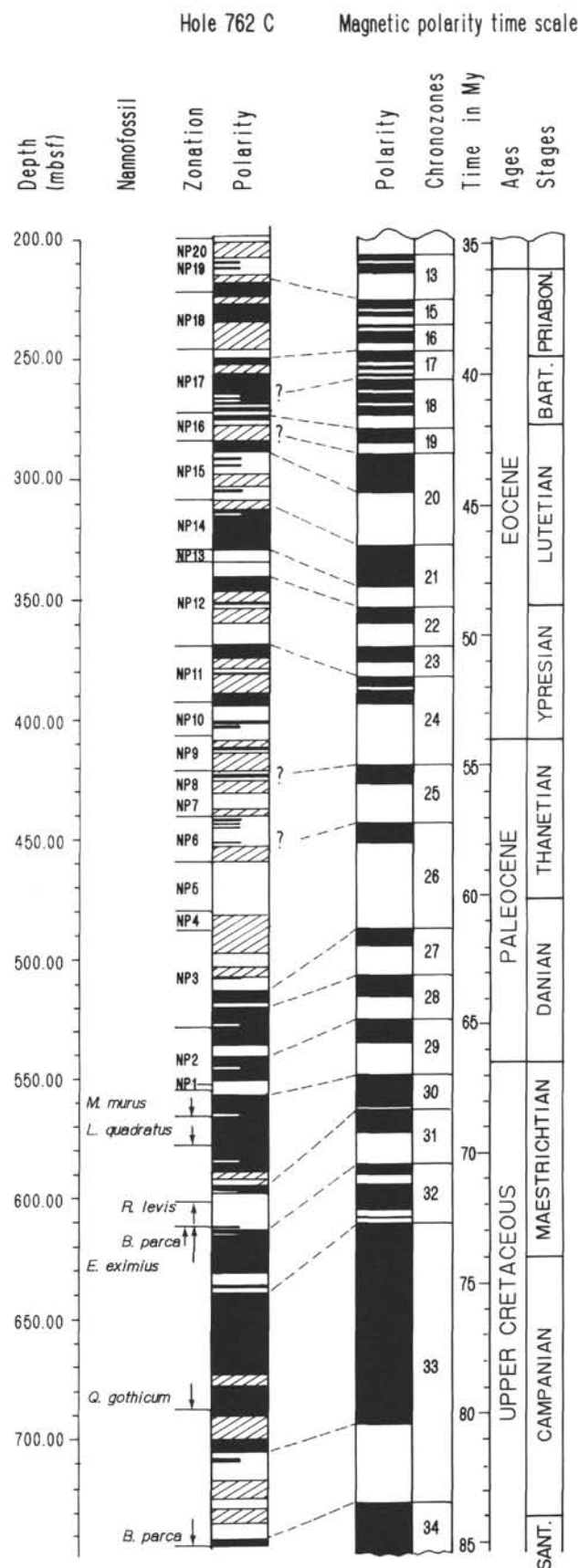


Figure 8. Comparison between the magnetostratigraphic results for Hole 762C, and the magnetic polarity time scale of Haq et al. (1987).

APPENDIX A

Direction of characteristic magnetization, Hole 761B, early Cenozoic-Late Cretaceous samples. The NRM column represents the initial NRM

intensity of each sample, the demagnetization step column refers to the highest step attained during the treatment of each sample.

Sample (core-section, cm)	Depth (mbsf)	NRM (A/m)	Inclination (°)	Demagnetization step	Sample (core-section, cm)	Depth (mbsf)	NRM (A/m)	Inclination (°)	Demagnetization step
122-761B-									
8H-1, 68	61.90	1.32 E-3	-44	100° + 30 mT	17X-6, 46	140.16	4.05 E-4	+51	100° + 25 mT
8H-1, 130	62.50	7.02 E-3	-8	100° + 35 mT	17X-6, 105	140.75	1.09 E-3	+59	300° + 32 mT
8H-2, 70	63.40	1.06 E-3	+25	100° + 30 mT	17X-7, 22	141.42	1.08 E-3	+52	100° + 26 mT
8H-2, 130	64.00	3.93 E-3	-8	100° + 35 mT	18X-1, 30	142.00	2.75 E-3	+69	500°
8H-3, 83	65.04	2.14 E-3	+27	100° + 30 mT	18X-2, 43	143.63	1.24 E-3	+48	35 mT
8H-3, 140	65.60	1.34 E-3	+6	100° + 35 mT	18X-3, 30	145.00	2.80 E-3	+69	450°
8H-4, 81	66.52	2.16 E-3	-1	100° + 30 mT	18X-4, 49	146.69	1.98 E-3	+62	500°
8H-4, 140	67.10	3.16 E-3	+14	100° + 35 mT	18X-5, 47	148.17	1.75 E-3	+54	100° + 35 mT
8H-5, 36	67.56	9.09 E-4	-21	100° + 30 mT	18X-5, 104	148.74	5.28 E-4	+55	300° + 32 mT
8H-5, 110	68.30	2.28 E-3	+18	100° + 35 mT	18X-6, 28	149.49	7.06 E-4	+65	500°
8H-6, 61	69.31	1.48 E-3	-10	100° + 35 mT	18X-6, 120	150.40	5.50 E-4	+62	300° + 32 mT
8H-6, 132	70.02	1.24 E-3	+17	100° + 30 mT	19X-1, 54	151.74	6.34 E-4	-65	100° + 26 mT
8H-7, 79	71.00	1.17 E-3	-27	100° + 30 mT	19X-1, 115	152.35	6.54 E-4	+53	300° + 32 mT
9H-1, 50	71.20	1.94 E-3	-36	100° + 35 mT	19X-2, 52	153.23	2.30 E-3	+56	500°
9H-1, 126	71.96	2.52 E-3	+17	100° + 25 mT	19X-3, 50	154.70	2.07 E-3	+54	450°
9H-2, 57	72.77	1.40 E-3	-25	100° + 35 mT	19X-4, 49	156.19	2.41 E-3	+50	35 mT
9H-2, 141	73.61	2.14 E-3	+26	100° + 30 mT	19X-5, 13	157.33	2.44 E-3	+44	450°
9H-3, 50	74.20	1.28 E-3	+50	100° + 35 mT	20X-1, 44	161.15	3.76 E-3	+36	100° + 40 mT
9H-3, 114	74.85	1.29 E-3	+29	100° + 25 mT	20X-1, 112	161.82	2.56 E-3	-47	100° + 29 mT
9H-4, 20	75.40	1.07 E-3	+14	100° + 35 mT	20X-2, 47	162.68	1.38 E-3	-67	100° + 26 mT
9H-4, 74	75.94	1.60 E-3	-27	100° + 30 mT	20X-3, 30	164.00	2.54 E-4	-59	100° + 26 mT
9H-5, 10	76.80	9.91 E-4	+60	100° + 29 mT	20X-4, 55	165.76	3.05 E-4	-57	450°
9H-5, 62	77.32	1.74 E-3	+22	100° + 25 mT	20X-4, 114	166.34	1.12 E-4	+15	100° + 29 mT
9H-6, 10	78.30	1.18 E-3	-40	100° + 29 mT	20X-5, 65	167.36	1.02 E-4	+50	450°
9H-6, 75	78.95	1.56 E-3	-36	100° + 28 mT	20X-5, 130	168.00	6.20 E-5	+70	300° + 25 mT
9H-7, 32	80.02	1.59 E-3	-52	100° + 28 mT	20X-6, 21	168.41	2.80 E-5	+54	300°
10H-1, 120	81.40	1.59 E-3	-40	100° + 28 mT	21X-1, 52	170.72	2.70 E-5	+58	100°
10H-2, 80	82.50	2.16 E-3	-41	100° + 28 mT	21X-1, 113	171.33	4.10 E-5	-34	100°
10H-3, 122	84.42	1.83 E-3	-44	100° + 28 mT	21X-2, 53	172.23	2.50 E-5	+65	100° + 15 mT
10H-4, 80	85.50	2.09 E-3	+13	100° + 22 mT	21X-2, 113	172.83	9.00 E-6	+52	100° + 10 mT
10H-5, 80	87.00	2.14 E-3	-39	100° + 22 mT	21X-3, 44	173.64	3.70 E-5	-40	100° + 14 mT
10H-6, 80	88.50	2.33 E-3	-44	100° + 22 mT	21X-3, 110	174.30	2.70 E-5	+72	100° + 18 mT
10H-7, 23	89.43	1.96 E-3	-44	100° + 28 mT	21X-4, 41	175.11	2.30 E-5	-65	100° + 18 mT
11X-1, 114	90.84	2.09 E-3	-32	100° + 28 mT	21X-4, 110	175.80	2.50 E-5	+55	100° + 14 mT
11X-2, 31	91.51	8.98 E-4	-59	100° + 28 mT	21X-5, 45	176.65	2.90 E-5	+55	100° + 18 mT
11X-3, 118	93.88	1.04 E-3	-14	100° + 28 mT	21X-5, 111	177.31	2.80 E-5	+31	100° + 18 mT
14X-1, 50	102.20	6.58 E-3	-36	100° + 29 mT	21X-6, 45	178.15	2.50 E-5	+32	100° + 18 mT
14X-1, 123	102.93	8.26 E-4	+41	100° + 20 mT	22X-1, 50	180.20	2.40 E-5	+52	100° + 18 mT
14X-2, 57	103.77	1.74 E-3	-47	100° + 29 mT	22X-1, 51	180.21	2.40 E-5	+49	100°
14X-2, 129	104.50	1.16 E-3	-42	100° + 25 mT	22X-2, 26	181.46	3.20 E-5	+24	100°
14X-3, 56	105.26	1.20 E-3	-43	100° + 20 mT	22X-2, 92	182.13	1.04 E-4	-56	300°
14X-4, 10	106.30	6.76 E-3	+20	100° + 20 mT	22X-3, 54	183.24	6.40 E-5	-64	300°
14X-4, 65	106.86	2.86 E-3	-34	100° + 25 mT	22X-3, 117	183.87	1.04 E-4	-75	100° + 25 mT
16X-1, 49	123.19	2.95 E-3	-26	100° + 25 mT	22X-4, 49	184.69	2.05 E-4	-76	100° + 26 mT
16X-1, 120	123.90	2.18 E-3	-41	100° + 29 mT	22X-4, 115	185.35	9.90 E-5	-56	100° + 25 mT
16X-2, 49	124.69	3.99 E-3	-77	100° + 25 mT	22X-5, 34	186.04	8.50 E-5	-65	100° + 15 mT
16X-3, 49	126.19	1.37 E-3	-75	100° + 25 mT	22X-5, 97	186.67	2.15 E-4	-62	100° + 32 mT
16X-4, 49	127.70	3.73 E-3	-36	100° + 25 mT	22X-6, 17	187.37	4.70 E-5	-65	100° + 15 mT
16X-4, 120	128.40	8.44 E-4	+49	100° + 29 mT	23X-1, 73	189.93	1.18 E-3	-82	500°
17X-1, 47	132.68	1.05 E-3	+12	100° + 25 mT	23X-1, 133	190.53	8.17 E-4	-65	100° + 32 mT
17X-1, 121	133.41	1.07 E-3	+38	300° + 32 mT	23X-2, 76	191.46	1.45 E-3	-69	35 mT
17X-2, 54	134.24	9.88 E-3	+58	100° + 25 mT	23X-2, 131	192.01	5.30 E-4	-60	100° + 32 mT
17X-2, 126	134.96	8.80 E-3	+51	300° + 32 mT	23X-3, 71	192.92	8.64 E-4	-84	500°
17X-3, 54	135.74	3.64 E-4	+67	100° + 25 mT	23X-3, 135	193.55	5.84 E-4	-75	100° + 32 mT
17X-3, 127	136.47	1.85 E-4	+68	100° + 29 mT	23X-4, 68	194.38	5.19 E-4	-10	100° + 32 mT
17X-4, 54	137.24	6.64 E-4	+62	100° + 25 mT	23X-5, 50	195.71	3.91 E-3	+25	100° + 35 mT
17X-5, 46	138.66	8.73 E-4	+55	100° + 25 mT	23X-5, 113	196.33	1.25 E-3	+63	100° + 32 mT
17X-5, 125	139.45	1.02 E-3	+59	300° + 32 mT	24X-1, 130	200.00	3.10 E-3	+38	100° + 26 mT

Appendix A (continued).

Sample (core-section, cm)	Depth (mbsf)	NRM (A/m)	Inclination (°)	Demagnetization step
122-761B-				
24X-2, 142	201.62	7.29 E-3	+55	100° + 40 mT
24X-3, 137	203.07	6.69 E-3	+59	35 mT
24X-4, 24	203.45	4.79 E-3	+31	500°
24X-4, 94	204.14	8.55 E-4	+65	100° + 32 mT
25X-1, 50	208.71	3.13 E-3	-17	500°
25X-2, 95	210.65	3.57 E-3	-65	100° + 25 mT
25X-3, 109	212.29	5.70 E-3	-55	500°
25X-4, 138	214.08	5.23 E-3	-75	100° + 35 mT
25X-5, 66	214.86	7.22 E-3	-37	35 mT

APPENDIX B

Direction of characteristic magnetization, Hole 762C, early Cenozoic–Late Cretaceous samples. The NRM column represents the initial NRM

intensity of each sample, the demagnetization step column refers to the highest step attained during the treatment of each sample.

Sample (core-section, cm)	Depth (mbsf)	NRM (A/m)	Inclination (°)	Demagnetization step	Sample (core-section, cm)	Depth (mbsf)	NRM (A/m)	Inclination (°)	Demagnetization step
122-762C-									
5X-1, 51	199.01	1.70 E-5	+46	100° + 15 mT	12X-6, 130	273.80	4.28 E-3	-14	100° + 40 mT
5X-1, 132	199.83	1.30 E-5	+71	100° + 10 mT	13X-1, 50	275.00	4.54 E-3	-24	100° + 42 mT
5X-2, 52	200.53	3.60 E-5	+32	100° + 10 mT	13X-1, 131	275.81	5.24 E-3	-48	100° + 40 mT
6X-1, 68	208.68	2.50 E-5	+54	100° + 15 mT	13X-2, 20	276.20	3.20 E-3	+40	100° + 42 mT
6X-1, 135	209.36	2.20 E-5	-35	100°	13X-2, 81	276.81	3.77 E-3	+45	100° + 42 mT
6X-2, 64	210.14	3.00 E-5	+46	100° + 10 mT	14X-1, 50	284.50	5.42 E-3	-40	100° + 42 mT
6X-2, 135	210.86	1.70 E-5	+1	100° + 15 mT	14X-1, 132	285.32	8.69 E-3	-7	100° + 40 mT
6X-3, 68	211.68	1.80 E-5	-48	100° + 10 mT	14X-2, 57	286.07	4.17 E-3	-14	100° + 42 mT
6X-3, 135	212.35	1.80 E-5	+13	100°	14X-2, 132	286.82	3.88 E-3	-36	100° + 45 mT
6X-4, 68	213.18	1.80 E-5	+58	100° + 10 mT	14X-3, 52	287.52	3.77 E-3	-5	100° + 42 mT
6X-4, 135	213.86	3.10 E-5	+46	100° + 10 mT	14X-3, 132	288.32	3.08 E-3	-8	100° + 35 mT
6X-5, 34	214.35	2.80 E-5	+48	100° + 10 mT	14X-4, 50	289.00	4.69 E-3	+33	100° + 35 mT
7X-1, 68	218.18	1.10 E-5	-58	100°	14X-4, 132	289.83	3.07 E-3	-2	100° + 40 mT
7X-1, 130	218.81	2.60 E-5	-65	100° + 10 mT	14X-5, 37	290.37	4.51 E-3	+47	100° + 35 mT
7X-2, 64	219.64	5.50 E-5	-77	100° + 15 mT	14X-5, 108	291.08	4.32 E-3	-31	100° + 35 mT
7X-2, 130	220.30	4.60 E-5	-45	100°	14X-6, 58	292.08	2.88 E-3	+26	100° + 35 mT
7X-3, 52	221.02	2.90 E-5	-68	100° + 10 mT	14X-6, 132	292.83	7.25 E-3	+26	100° + 35 mT
7X-3, 106	221.56	2.10 E-5	-50	100°	15X-1, 30	293.80	5.33 E-3	-30	100° + 35 mT
7X-4, 63	222.63	9.00 E-6	-34	100°	15X-1, 139	294.90	4.21 E-3	+24	100° + 35 mT
7X-4, 130	223.30	3.20 E-5	-54	100°	15X-2, 31	295.31	4.64 E-3	+12	100° + 35 mT
8X-1, 50	227.50	1.20 E-5	-33	100°	15X-2, 109	296.10	4.41 E-3	-8	100° + 35 mT
8X-1, 127	228.27	1.50 E-5	—		15X-3, 52	297.02	4.43 E-3	+21	100° + 35 mT
8X-2, 130	229.80	3.60 E-5	-70	100° + 10 mT	16X-1, 50	303.50	3.94 E-3	+8	100° + 35 mT
8X-3, 94	230.94	4.30 E-5	-65	100° + 10 mT	16X-1, 127	304.27	5.12 E-3	-22	100° + 35 mT
8X-4, 128	232.78	4.90 E-5	-67	100° + 10 mT	16X-2, 50	305.00	3.02 E-3	+47	100° + 35 mT
8X-5, 47	233.47	1.30 E-5	-64	100° + 10 mT	16X-2, 124	305.75	3.59 E-3	-3	100° + 35 mT
9X-1, 25	236.75	2.70 E-5	—		16X-3, 50	306.50	3.07 E-3	+31	100° + 35 mT
10X-1, 50	246.50	1.00 E-5	+47	100° + 10 mT	16X-3, 121	307.22	4.06 E-3	+16	100° + 35 mT
10X-1, 130	247.30	2.50 E-5	+64	100°	16X-4, 16	307.67	5.50 E-3	+12	100° + 35 mT
10X-2, 57	248.07	1.90 E-5	+47	100° + 15 mT	17X-1, 25	312.76	4.05 E-3	-33	100° + 35 mT
10X-2, 129	248.80	2.70 E-5	+69	100°	17X-1, 130	313.80	2.61 E-3	+7	100° + 35 mT
10X-3, 41	249.41	3.30 E-5	-61	100° + 10 mT	17X-2, 131	315.31	7.20 E-3	-39	100° + 35 mT
10X-3, 101	250.02	4.70 E-5	-28	100°	17X-3, 87	316.37	4.76 E-3	-9	100° + 40 mT
10X-4, 43	250.93	3.80 E-5	-56	100° + 10 mT	17X-4, 23	317.23	4.06 E-3	-35	100° + 35 mT
10X-4, 101	251.51	4.20 E-5	-73	100° + 10 mT	17X-5, 137	319.87	4.12 E-3	-24	100° + 40 mT
11X-1, 68	256.18	2.86 E-3	-43	100° + 45 mT	18X-1, 50	322.50	3.85 E-3	-7	100° + 35 mT
11X-1, 129	256.79	3.18 E-3	-8	100° + 40 mT	18X-2, 50	324.00	4.14 E-3	-33	100° + 35 mT
11X-2, 57	257.57	2.12 E-3	-17	100° + 45 mT	18X-3, 50	325.50	3.32 E-3	-18	100° + 35 mT
11X-2, 129	258.29	3.73 E-3	-41	100° + 40 mT	18X-4, 50	327.00	2.56 E-3	-11	100° + 40 mT
11X-3, 60	259.10	2.07 E-3	-17	100° + 40 mT	18X-4, 110	327.60	4.12 E-3	-38	100° + 35 mT
11X-3, 129	259.79	3.13 E-3	-7	100° + 30 mT	18X-5, 50	328.50	3.65 E-3	+20	100° + 40 mT
11X-4, 68	260.68	2.06 E-3	-25	100° + 45 mT	18X-6, 50	330.00	3.53 E-3	+18	100° + 40 mT
11X-4, 129	261.29	3.23 E-3	-26	100° + 30 mT	19X-1, 89	332.39	3.96 E-3	+16	100° + 35 mT
11X-5, 68	262.18	3.31 E-3	-37	100° + 45 mT	19X-2, 30	333.30	4.04 E-3	+19	100° + 40 mT
11X-5, 129	262.79	3.44 E-3	-19	100° + 40 mT	19X-3, 30	334.80	4.18 E-3	+11	100° + 40 mT
11X-6, 68	263.68	2.55 E-3	-27	100° + 45 mT	19X-4, 88	336.80	3.20 E-3	+25	100° + 40 mT
11X-6, 129	264.29	5.09 E-3	-10	100° + 35 mT	19X-5, 30	337.80	5.71 E-3	+8	100° + 40 mT
12X-1, 53	265.53	2.76 E-3	+15	100° + 45 mT	20X-1, 52	341.52	2.91 E-3	-23	100° + 32 mT
12X-1, 119	266.19	6.02 E-3	-35	100° + 40 mT	20X-1, 131	342.52	5.45 E-3	-42	100° + 45 mT
12X-2, 50	267.00	2.21 E-3	+31	100° + 42 mT	20X-2, 112	343.62	1.63 E-4	-39	100° + 25 mT
12X-2, 119	267.70	4.01 E-3	-8	100° + 40 mT	20X-3, 131	345.31	1.77 E-4	-75	100° + 35 mT
12X-3, 68	268.68	3.64 E-3	-36	100° + 42 mT	20X-4, 55	346.05	8.00 E-5	-46	100° + 25 mT
12X-3, 130	269.31	4.38 E-3	+7	100° + 40 mT	21X-1, 47	350.97	4.47 E-3	-55	100° + 32 mT
12X-4, 60	270.10	2.38 E-3	+1	100° + 42 mT	21X-1, 107	351.57	4.49 E-3	-34	100° + 45 mT
12X-4, 130	270.81	3.47 E-3	-17	100° + 40 mT	21X-2, 22	352.22	5.18 E-3	+3	100° + 32 mT
12X-5, 60	271.60	3.13 E-3	-35	100° + 42 mT	21X-2, 64	352.65	9.11 E-3	+41	100° + 40 mT
12X-5, 130	272.30	3.28 E-3	+4	100° + 40 mT	22X-1, 134	361.34	5.60 E-5	+72	250°
12X-6, 61	273.11	2.07 E-3	+22	100° + 42 mT	22X-2, 138	362.88	2.60 E-5	+64	250°

B. GALBRUN

Appendix B (continued).

Sample (core-section, cm)	Depth (mbsf)	NRM (A/m)	Inclination (°)	Demagnetization step	Sample (core-section, cm)	Depth (mbsf)	NRM (A/m)	Inclination (°)	Demagnetization step
122-762C-					122-762C-				
22X-3, 128	364.28	1.40 E-5	+75	300°	33X-2, 129	462.29	1.70 E-5	+73	200°
22X-4, 107	365.57	1.33 E-4	+73	300°	33X-3, 129	463.79	8.00 E-6	+64	250°
22X-5, 122	367.23	1.58 E-4	+59	40 mT	33X-4, 129	465.29	8.00 E-6	+35	100°
22X-6, 27	367.77	4.20 E-5	+76	100° + 10 mT	33X-5, 129	466.79	1.20 E-5	+57	100°
22X-6, 80	368.31	1.12 E-5	-5	100° + 25 mT	34X-1, 125	470.25	1.50 E-5	+77	200°
23X-1, 132	370.82	5.25 E-5	-52	40 mT	34X-2, 78	471.28	4.00 E-6	+61	200°
23X-2, 113	372.13	2.04 E-5	-65	300°	34X-3, 135	473.35	1.90 E-5	+62	200°
23X-3, 19	372.69	4.05 E-5	-15	100° + 20 mT	34X-4, 66	474.16	6.00 E-6	+71	200°
23X-CC,33	373.83	5.30 E-4	-66	300°	34X-5, 84	475.84	1.30 E-5	+72	200°
24X-1, 59	379.59	3.00 E-5	+3	100°	34X-5, 93	475.93	1.40 E-5	+28	100°
24X-1, 124	380.24	1.70 E-5	+40	200°	35X-1, 60	479.10	2.50 E-5	+16	100°
24X-CC,24	380.64	3.10 E-5	-40	150°	35X-2, 67	480.68	5.00 E-6	+61	200°
25X-1, 108	389.58	8.20 E-5	-61	300°	35X-2, 108	481.08	1.40 E-5	—	
25X-2, 137	391.37	3.90 E-5	-41	200°	37X-1, 60	498.11	9.90 E-5	+75	100° + 30 mT
25X-3, 135	392.85	8.50 E-5	-59	20 mT	37X-2, 42	499.42	1.60 E-5	+12	100°
25X-4, 139	394.40	4.10 E-5	-78	150°	37X-3, 32	500.82	2.10 E-5	—	
25X-5, 26	394.76	3.90 E-5	+31	100° + 10 mT	37X-4, 52	502.52	1.30 E-5	+46	100°
26X-1, 67	398.67	2.18 E-4	+26	100° + 10 mT	38X-1, 82	507.82	3.00 E-5	-10	100°
26X-1, 138	399.38	2.10 E-5	+49	250°	38X-2, 138	509.88	1.10 E-5	+28	100°
26X-2, 65	400.15	3.90 E-5	+42	100°	38X-3, 52	510.53	2.60 E-5	+40	100° + 10 mT
26X-2, 143	400.93	5.20 E-5	-66	100° + 10 mT	38X-3, 142	511.42	2.00 E-5	+2	100°
26X-3, 69	401.69	9.00 E-6	-41	100°	38X-4, 62	512.12	3.50 E-5	+73	100°
26X-3, 137	402.37	6.90 E-5	+43	100° + 10 mT	38X-5, 82	513.83	4.50 E-5	-20	100° + 10 mT
26X-4, 43	402.93	2.70 E-5	+70	100°	38X-6, 64	515.14	1.20 E-5	—	
26X-4, 93	403.43	4.40 E-5	-21	100°	38X-7, 18	516.18	6.70 E-5	-39	100° + 10 mT
27X-1, 140	403.90	6.00 E-5	+78	100° + 10 mT	39X-1, 136	517.86	9.10 E-5	-56	200°
27X-2, 138	405.38	1.80 E-5	+62	250°	39X-2, 61	518.60	4.40 E-5	+23	100° + 15 mT
27X-3, 108	406.58	2.00 E-5	+83	250°	39X-2, 137	519.37	6.30 E-5	+36	300°
27X-4, 106	408.06	2.20 E-5	+60	250°	39X-3, 30	519.80	2.10 E-5	-60	100° + 15 mT
27X-4, 128	408.28	1.80 E-5	+65	100°	39X-3, 94	520.44	7.70 E-5	-32	25 mT
28X-1, 28	412.29	9.20 E-5	-66	100° + 10 mT	39X-4, 68	521.68	3.80 E-5	-47	100°
28X-1, 127	413.27	2.80 E-5	+43	100°	39X-4, 130	522.30	7.20 E-5	-35	250°
28X-CC,28	413.88	2.90 E-5	—		39X-5, 62	523.12	4.10 E-5	-37	100° + 10 mT
29X-1, 48	421.98	8.00 E-6	+17	100°	39X-5, 137	523.87	1.42 E-4	-31	28 mT
29X-1, 144	422.94	4.10 E-5	-26	100° + 10 mT	40X-1, 40	526.40	5.00 E-5	-61	100° + 10 mT
29X-2, 108	424.09	3.10 E-5	-28	100°	40X-1, 113	527.13	8.90 E-5	+39	250°
29X-3, 30	424.80	8.00 E-6	+15	100°	40X-2, 57	528.07	4.10 E-5	-57	100°
29X-3, 67	425.18	2.80 E-5	+70	300°	40X-2, 142	528.92	1.70 E-4	-66	250°
30X-1, 58	431.58	1.70 E-5	+73	250°	40X-3, 143	530.43	9.00 E-4	-74	150°
30X-2, 103	433.53	9.20 E-5	+23	100° + 25 mT	40X-4, 138	531.88	1.11 E-4	-48	150°
30X-3, 116	435.16	3.70 E-5	+44	100° + 10 mT	40X-5, 123	533.23	1.04 E-4	-47	150°
30X-CC,42	436.62	4.00 E-6	+73	200°	40X-6, 134	534.85	1.18 E-4	-58	28 mT
31X-1, 30	440.80	1.70 E-5	+55	100°	41X-1, 53	536.03	2.60 E-5	—	
31X-1, 104	441.55	1.70 E-5	-71	100°	41X-1, 141	536.92	4.70 E-5	+23	250°
31X-2, 37	442.37	2.10 E-5	+35	100°	41X-2, 50	537.50	3.10 E-5	—	
31X-2, 109	443.09	1.90 E-5	-57	100°	41X-2, 136	538.36	1.50 E-5	+21	100°
31X-3, 53	444.03	2.80 E-5	+57	100° + 10 mT	41X-3, 147	539.98	2.50 E-5	+49	100° + 10 mT
31X-3, 135	444.86	1.50 E-5	-64	100°	41X-4, 53	540.53	2.90 E-5	-62	100°
31X-4, 58	445.58	2.90 E-5	+39	100° + 10 mT	41X-4, 110	541.11	2.50 E-5	-56	100°
31X-4, 131	446.32	3.50 E-5	+46	300°	41X-5, 115	542.65	5.00 E-5	-46	100° + 10 mT
31X-5, 130	447.80	7.00 E-6	+71	300°	41X-6, 105	544.05	9.40 E-5	-19	100° + 30 mT
31X-6, 28	448.28	7.00 E-6	+70	200°	41X-6, 140	544.40	3.50 E-5	-64	100° + 10 mT
31X-6, 119	449.19	1.10 E-5	+16	100°	42X-1, 42	542.42	1.60 E-5	-67	100° + 10 mT
32X-1, 52	450.52	4.00 E-6	+29	100°	42X-1, 87	545.87	8.00 E-6	+44	100° + 10 mT
32X-1, 139	451.39	7.00 E-6	-65	100°	42X-2, 48	546.98	8.80 E-5	-63	100° + 15 mT
32X-2, 50	452.00	1.40 E-5	+23	100°	42X-2, 96	547.46	2.90 E-5	-48	100°
32X-2, 109	452.59	2.20 E-5	—		42X-3, 40	548.40	3.80 E-5	-64	100°
33X-1, 54	460.04	7.00 E-6	+5	100°	42X-3, 132	549.32	3.80 E-5	-65	100° + 10 mT
33X-1, 129	460.79	6.00 E-6	+69	200°	42X-4, 70	550.21	4.20 E-5	-53	100° + 10 mT

Appendix B (continued).

Sample (core-section, cm)	Depth (mbsf)	NRM (A/m)	Inclination (°)	Demagnetization step	Sample (core-section, cm)	Depth (mbsf)	NRM (A/m)	Inclination (°)	Demagnetization step
122-762C-									
42X-4, 80	550.30	4.50 E-5	-58	100° + 10 mT	49X-3, 109	615.59	2.13 E-4	-54	100° + 25 mT
42X-5, 75	551.76	3.80 E-5	-2	100°	49X-4, 50	616.50	3.40 E-5	-49	100° + 5 mT
42X-5, 130	552.30	4.40 E-5	+11	100° + 15 mT	49X-4, 111	617.11	4.90 E-5	-59	100° + 20 mT
42X-6, 25	552.75	8.20 E-5	+6	100° + 10 mT	49X-5, 41	617.91	5.10 E-5	-63	100° + 20 mT
42X-6, 136	553.86	1.00 E-4	+29	100° + 20 mT	49X-5, 108	618.58	4.10 E-5	-59	100° + 5 mT
43X-1, 41	554.91	2.50 E-5	+41	100° + 20 mT	50X-1, 47	621.47	5.80 E-3	-15	100° + 25 mT
43X-1, 100	555.50	6.60 E-5	+53	100° + 25 mT	50X-1, 113	622.14	2.20 E-2	-44	100° + 40 mT
43X-2, 50	556.50	2.50 E-5	+20	100° + 10 mT	50X-2, 102	623.52	5.52 E-4	-58	100° + 40 mT
43X-2, 110	557.10	1.80 E-5	-40	100°	50X-3, 98	624.98	1.51 E-2	-55	100° + 40 mT
43X-3, 42	557.92	5.87 E-4	-55	100° + 25 mT	50X-4, 104	626.54	1.81 E-4	-59	100° + 30 mT
43X-3, 141	558.91	1.90 E-5	-18	100°	50X-5, 47	627.47	4.12 E-4	-56	100° + 40 mT
43X-4, 20	559.20	2.70 E-5	-12	100°	50X-6, 121	629.71	4.07 E-4	-66	500°
43X-4, 113	560.13	1.50 E-5	-22	100°	50X-7, 37	630.38	1.78 E-4	-69	100° + 40 mT
43X-5, 22	560.72	1.30 E-5	+3	100°	51X-1, 58	631.08	6.68 E-4	-46	100° + 25 mT
43X-5, 96	561.46	3.50 E-5	-23	100°	51X-1, 135	631.87	3.38 E-3	+38	100° + 40 mT
44X-1, 51	564.51	4.00 E-5	-59	100° + 5 mT	51X-2, 141	633.41	1.10 E-3	+41	100° + 40 mT
44X-1, 132	565.32	5.50 E-5	+52	300°	51X-3, 117	634.67	1.31 E-4	+68	100° + 40 mT
44X-2, 52	566.02	5.90 E-5	-56	100° + 10 mT	51X-4, 42	635.42	1.92 E-4	+70	100° + 25 mT
44X-2, 132	566.83	1.06 E-4	-76	300°	51X-4, 135	636.35	7.53 E-3	-30	35 mT
44X-3, 126	568.26	1.13 E-4	-46	300°	51X-5, 44	636.94	1.16 E-2	-23	100° + 35 mT
44X-4, 95	569.45	1.16 E-4	-49	250°	51X-5, 133	637.84	1.09 E-2	+8	100° + 30 mT
44X-5, 102	571.02	3.98 E-4	-62	60 mT	51X-6, 43	638.43	1.40 E-2	+8	100° + 25 mT
44X-6, 67	572.17	1.07 E-4	-44	250°	51X-6, 112	639.13	1.03 E-2	-32	100° + 30 mT
45X-1, 29	573.79	1.37 E-4	-61	350°	52X-1, 117	641.17	1.84 E-2	-75	100° + 25 mT
45X-2, 112	576.12	8.80 E-5	-58	100° + 20 mT	52X-2, 122	642.72	1.63 E-2	-54	150° + 40 mT
45X-3, 86	577.36	1.32 E-4	-65	300°	52X-3, 114	644.14	2.04 E-2	-54	500°
45X-4, 60	578.60	8.30 E-4	-23	100° + 15 mT	52X-4, 141	645.91	1.77 E-2	-71	150° + 40 mT
45X-4, 111	579.11	4.00 E-5	-32	100° + 15 mT	52X-5, 142	647.42	1.64 E-2	-38	150° + 30 mT
45X-5, 24	579.74	3.40 E-5	-13	100° + 25 mT	52X-6, 138	648.88	1.75 E-2	-45	150° + 30 mT
45X-5, 110	580.60	6.80 E-5	-64	100° + 20 mT	53X-1, 144	650.94	6.62 E-3	-19	100° + 40 mT
46X-1, 44	583.44	1.47 E-4	-61	300°	53X-2, 126	652.26	1.23 E-2	-70	150° + 30 mT
46X-1, 120	584.20	3.60 E-5	-9	100° + 10 mT	53X-3, 139	653.89	9.18 E-3	-82	150° + 30 mT
46X-2, 41	584.91	2.50 E-5	+34	100° + 10 mT	53X-4, 105	655.05	1.32 E-2	-44	150° + 30 mT
46X-2, 117	585.67	2.80 E-5	-42	100° + 10 mT	53X-5, 117	656.67	2.42 E-2	-46	500°
46X-3, 45	586.45	5.40 E-5	-44	100° + 20 mT	53X-6, 133	658.33	1.58 E-2	-46	150° + 30 mT
46X-3, 117	587.17	4.00 E-5	-52	100° + 10 mT	54X-1, 86	659.86	1.73 E-3	-42	100° + 30 mT
46X-4, 38	587.88	1.80 E-5	-49	100°	54X-2, 141	661.91	1.22 E-3	-58	60 mT
46X-4, 114	588.64	5.20 E-5	-57	100° + 15 mT	54X-3, 108	663.08	2.66 E-2	-52	100° + 40 mT
47X-1, 44	592.94	7.20 E-5	+55	300°	54X-4, 137	664.87	3.93 E-2	-53	150° + 30 mT
47X-2, 101	593.51	2.20 E-5	+18	100°	54X-5, 94	665.94	7.49 E-4	-76	150° + 30 mT
47X-3, 43	595.93	1.91 E-4	-16	100° + 25 mT	54X-6, 59	667.09	4.70 E-4	-66	150° + 30 mT
47X-3, 95	596.45	4.70 E-5	-73	100°	55X-1, 83	669.33	4.21 E-4	-68	150° + 30 mT
47X-4, 48	597.48	3.00 E-5	-34	100°	55X-2, 105	671.05	3.99 E-4	-67	150° + 30 mT
47X-4, 112	598.12	5.00 E-5	-62	100°	55X-3, 135	672.85	2.73 E-3	-79	500°
47X-5, 46	598.96	2.00 E-5	+75	100° + 25 mT	56X-1, 96	678.96	5.45 E-4	-75	150° + 30 mT
47X-5, 101	599.51	5.50 E-5	+63	350°	56X-2, 121	680.71	4.29 E-4	-74	150° + 30 mT
47X-6, 40	600.40	2.40 E-5	+83	300°	56X-3, 130	682.30	9.38 E-3	-39	50 mT
48X-1, 54	602.54	1.60 E-5	+80	300°	56X-4, 137	683.87	4.83 E-3	-63	150° + 30 mT
48X-2, 36	603.86	3.40 E-5	+58	300°	56X-5, 68	684.68	8.13 E-4	-59	150° + 30 mT
48X-3, 30	605.30	1.40 E-5	+67	300°	56X-6, 91	686.41	6.70 E-4	-69	150° + 30 mT
48X-4, 65	607.15	8.10 E-5	+67	450°	57X-1, 135	688.85	4.27 E-3	-42	100° + 30 mT
48X-5, 131	609.31	4.80 E-5	+63	100° + 40 mT	57X-2, 120	690.20	9.35 E-4	-68	150° + 30 mT
48X-6, 47	609.97	1.19 E-4	+63	50 mT	58X-3, 115	701.15	5.51 E-4	-63	100° + 60 mT
48X-7, 30	611.31	3.80 E-5	+66	100° + 40 mT	58X-4, 35	701.85	2.86 E-4	-70	150° + 30 mT
49X-1, 48	611.98	2.10 E-5	-24	100°	58X-5, 33	703.34	4.88 E-4	-68	150° + 30 mT
49X-1, 118	612.68	1.90 E-5	+52	100° + 25 mT	58X-6, 22	704.72	2.28 E-4	-60	100° + 20 mT
49X-2, 45	613.45	6.09 E-4	-51	100° + 25 mT	59X-1, 65	707.15	7.30 E-5	+31	100° + 20 mT
49X-2, 117	614.17	5.60 E-5	-40	100° + 5 mT	59X-2, 61	708.61	6.20 E-5	-67	100° + 5 mT
49X-3, 46	614.96	1.59 E-4	+53	100° + 25 mT	59X-3, 67	710.17	1.35 E-4	+69	100° + 25 mT

Appendix B (continued).

Sample (core-section, cm)	Depth (mbsf)	NRM (A/m)	Inclination (°)	Demagnetization step
122-762C-				
59X-4, 73	711.73	1.44 E-4	+54	100° + 25 mT
59X-5, 57	713.07	1.38 E-4	+71	100° + 25 mT
59X-6, 44	714.44	1.19 E-4	+31	100° + 25 mT
60X-1, 32	716.32	3.26 E-4	+71	500°
61X-1, 128	726.78	2.98 E-4	+78	40 mT
61X-2, 97	727.97	1.65 E-4	+71	150° + 30 mT
62X-1, 44	735.44	7.30 E-5	+74	150° + 30 mT
62X-2, 107	737.57	1.68 E-4	+75	150° + 30 mT
62X-3, 118	739.18	2.42 E-4	+61	100° + 50 mT
62X-4, 160	741.10	1.60 E-4	+71	100° + 30 mT
62X-5, 107	742.07	4.93 E-4	-63	500°